Visualization Method Based Stiffness Sensing System for Endoscopes

Visualization method based stiffness sensing system for endoscopes

Takanobu Iwai, Toshio Koyama, Hiroyuki Kagawa, Takeshi Yoneyama, and Tetsuyou Watanabe,
Member, IEEE

***Abstract*— This research developed novel stiffness sensing system attachable to endoscope. The system is an extension of our previous force sensing systems utilizing force visualization mechanism. The sensing part is attached to endoscopes. The force is visualized at the sensing part, and can be measured as visual information via endoscopes. The sensing part also has a structure of limiting the pressing amount. By measuring force at the limitation, the stiffness can be measured. The developed sensing part has the features of no electrical components, disposable, simple, easy sterilization, MRI-compatibility, and low-cost. The validation of the system was experimentally shown.**

I. Introduction

Endoscope is a powerful medical instrument. Via endoscope, medical doctors can minimal-invasively examine deep area where doctors cannot see directly. It is used for not only medical checks but also surgeries. However endoscope provides only visual information. If doctors can have not only visual but also haptic information, more accurate diagnosis can be expected. For example, palpation is a useful method for diagnosis at small hospitals and clinics. The tactile information in abdomen surgeries is very important to detect the difference between normal tissues and tumors. With this in mind, at our previous papers [1, 2], we developed force sensing system attachable to fiberscopes/endoscopes. By applying force visualization mechanism utilizing a highly elastic material (panty stocking fabric), the force sensing system has the very good features of high resolution, small size, low cost, no electrical part, and disposable of sensing part. However, the really required functions to detect affected area are to measure not only force but also stiffness or softness of tissues. With this in mind, this paper presented a novel stiffness sensing system that can be attached to endoscope. The main features are as follows:

Visualization mechanism based sensing system attachable to endoscope: The developed stiffness sensing system is an extension of our force sensing system [1, 2]. The sensing part is attached to endoscopes. The force or displacement are visualized at the sensing part, and can be measured as visual information. The sensing part has the features of no electrical component, disposable, simple, easy sterilization, MRI-compatibility, and low-cost.

Stiffness sensing: The sensing part has a structure of limiting the pressing amount. By measuring force at the limitation, the stiffness can be measured.

There are many kinds of force and tactile sensors for medical usage [1-7]. Most force and tactile sensors require electrical components, and are not easy to sterilize or disinfect. Additionally, amplifiers are required and the size and cost of the overall system is then large. Sensors without electrical components are suitable in the medical field. Concerning this, several force sensors without electric components have been developed, utilizing force visualization [8], pneumatic actuator [9], and optical fibers [10]. However, stiffness was not the target and cannot be measured. Only Kawahara et al. [11] developed a system to measure the stiffness of an organ utilizing air jet and camera. Drawbacks are not simple (requiring multiple endoscope-like systems) and largeness of overall system.

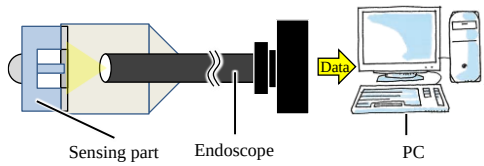

Figure 1. Ovewview of stiffness sensing system

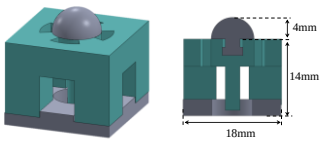

Figure 2. Schematic views of sensing part and its cross-selction

II. Structure and Mechanism

Fig. 1 shows the overview of the developed stiffness sensing system. If the sensing part makes a contact with an object or an organ, the image change associated with force/load and displacement is captured by camera equipped with the endoscope, and analyzed by PC. The sensing part has a structure of limiting the pressing amount, and by sensing force at the limitation, the stiffness information of the object or organ can be obtained.

A. Structure of sensing part

The schematic views of sensing part and its cross-section are shown in Fig. 2. The sensing part is constructed by head, spring, and base parts, shown in Fig. 3 (left). These three parts are connected by fitting. Spring part is made of silicone produced by Shin-etsu Silicone Company (silicone: KE-1308, hardener: CAT1300L-3, hardener volume: 6 %, see [12, 13]

T. Iwai and T Koyama are with the Department of mechanical Engineering, College of science and engineering, Kanazawa University, Ishikawa, Japan (corresponding author to provide e-mail: iwai.t@stu.kanazawa-u.ac.jp).

H. Kagawa, T. Yoneyama, and T. Watanabe is with the Institute of Science and Engineering, Kanazawa University, Kakuma-machi, Kanazawa, 9201192 Japan (e-mail: kagawa@t.kanazawa-u.ac.jp; yoneyama@t.kanazawa-u.ac.jp; te-watanabe@ieee.org).

for stiffness information), and Head and base parts (ABS plus: Young's Modulus: 2.2 [GPa]) were made by 3D printer (Stratasys Uprint SE). Fig. 3 (right) shows the manufactured one. If the head part makes a contact with an object or organ, the spring part deforms and the pin displaces according to the deformation. By capturing the displacement of the pin via camera, force or displacement can be estimated.

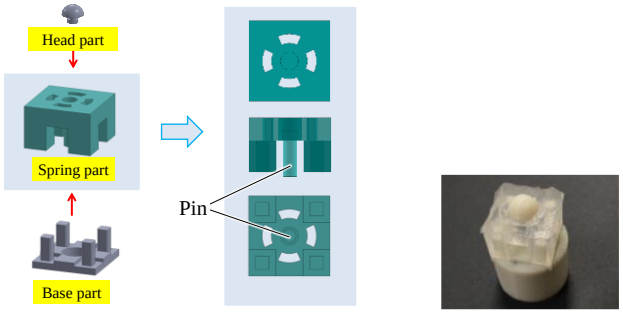

Figure 3. Components of sensing part (left) and Manufactured one(right)

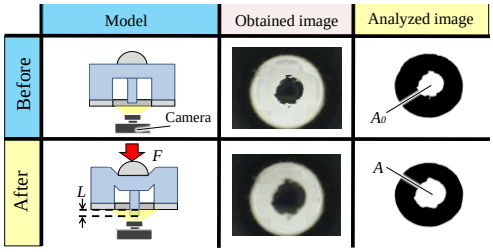

Figure 4. Principle for sensing force in the longitudinal direction of pin

B. *Principle for sensing force*

Before describing the principle for stiffness sensing, the principle for force sensing is described. The method to detect the displacement of pin is the same as the method presented in our previous papers [1, 2]. The difference is the structures for displacing pin according to load and for limiting the displacement for sensing stiffness. Three-axis force can be measured in principle. Because the main target is stiffness sensing in this paper, we focus on the measurement of force in the longitudinal direction of the pin. Fig. 4 shows the principle. If load F is applied to the head part, the pin displaces according to the deformation of the spring part. Then, the captured area for the pin changes from A_0 (initial area without load) to A, as seen in Fig. 4. Therefore, the load F can be derived from $A - A_0$ if we know the relation between F and $A - A_0$.

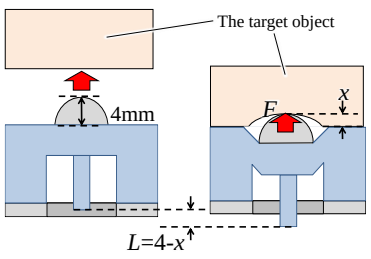

Figure 5. Principle for sensing stiffness

C. *Principle for sensing stiffness*

We defined that stiffness is F/x [N/mm] when the load F[N] is applied to the head part, and the target object deforms with the displacement (x [mm]) of the head part due to the load, as seen in Fig. 5. We assumed that the surface of target object around contact area is flat. Now, suppose the case of pressing a target object with the sensing part. If the surface of target object reaches the top surface of spring part, the increasing rate of the pressing distance/amount changes. We call the point change point P_c. By detecting the change point P_c and sensing load F at the point, load F when pressing the target object by exactly 4 [mm] can be obtained. Note that 4 [mm] is the height of the head part from the top surface of the spring part. Therefore, the stiffness can be derived from the relation between the F [N] and 4 [mm]. Note that because 4 [mm] does not always equal to the displacement of the head part, the displacement (x [mm]) has to be derived from the pin displacement $L\ (= 4 - x)$. L can be derived from $A - A_0$, similarly to the deviation of F.

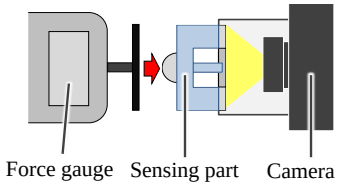

Figure 6. Schematic view of experimental setup for evaluating properties of sensing parts.

III. Experimental Evaluation

A. *Properties of sensing parts*

Fig. 6 shows the schematic view of experimental setup for evaluating the properties of sensing part. The sensing part was attached to the camera (Elecom UCAM-DLT30HSV: resolution: 640×480 [pixel]), and fixed. Note that here the camera instead of endoscope was used for easy setup. Force gauge (IMADA DS2-500N) was attached to the automatic positioning stage (IMADA MX2-500N). The flat plate was attached to the tip of the force gauge. By moving the force gauge, we pressed the head part of the developed sensing part with the flat plate. Initially it is set that the palate was in contact with the sensing part with the force value of 0.00 [N]. Then, the automatic positioning stage was controlled to increase the magnitude of the load by 0.25 [N], until the load reached 5.00 [N]. At every step, the value of force gauges and the moving distance of automatic positioning stage were recorded, and photo was taken by the camera to obtain the area for the pin A.

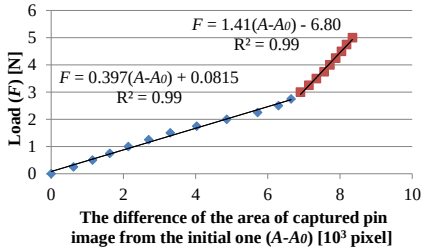

Figure 7. Load F [N] v.s. the difference of the area of captured pin image from the initial one ($A - A_0$)

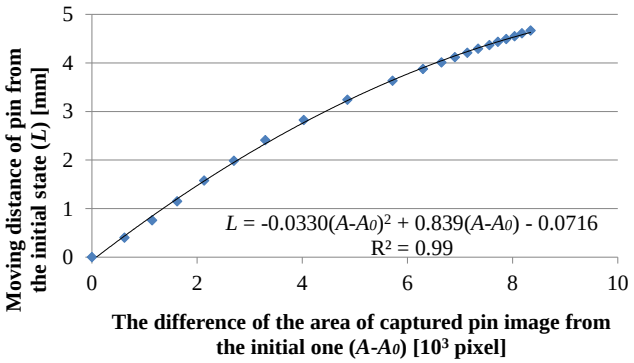

Figure 8. Moving distance of pin from the initial state L [mm] v.s. the difference of the area of captured pin image from the initial one ($A - A_0$)

Fig. 7 shows the obtained relation between load F [N] and the difference of the area of captured pin image from the initial one ($A - A_0$). It is seen that load F linearly increases with the increase of $A - A_0$. However, around $A - A_0 = 7 \times 10^3$ [pixel] the increasing rate of load F suddenly changed. This change is due to the occurrence of contact between the plate and (the top surface of) the spring part. Two regression curves were obtained by dividing the data taking the change as boundary. Each regression curve corresponds to the data for $L = 0 \sim 4$ [mm] and for $L = 4 \sim$ [mm]. The obtained regression curves are shown in Fig. 7 with the coefficient of determination. It is seen that a linear function can represent the relation very well.

Fig. 8 shows the relation between L and $A - A_0$. The quadratic function was used for regression. It is seen that a quadratic function can represent the relation very well.

B. Sensing stiffness of soft objects

By utilizing the relations obtained at the previous subsection (see Fig. 7 and Fig. 8), we tried to sense the stiffness of soft objects. The procedure of sensing stiffness is as follows:

Step1: Detect **the point P_c where an object makes a contact with the top surface of the spring part**. $A - A_0$ at the point P_c is derived.

Step 2: The load F and the moving distance of pin from the initial state L [mm] at the point P_c were derived, utilizing $A - A_0$ and the regression curves shown in Fig. 7 and Fig.8.

Step 3: Derive the displacement of the head part from the initial stage x [mm] at the point P_c, by $L = 4 - x$.

Step 4: Derive the stiffness F/x [N/mm].

If increasing pushing force against soft objects with the step of a certain value (for example, 0.25 [N]), the increasing rate of the pushing distance/amount or $A - A_0$ suddenly changes due to the contact between the object and the top surface of spring part. P_c at step 1 is the point at the change, and can be detected by detecting the change (Note that practical method for the detection will be described later).

Fig. 9 shows the schematic view of experimental setup to validate the developed stiffness sensing system. The experimental system is the same as the one shown in Fig. 6, except that a soft object is attached to the plate as a target object. We used two target objects made of silicone and melamine foam. The shape for these objects was cylinder with the height of 11 [mm] and the radius of 11 [mm]. The stiffness properties for the soft objects are experimentally obtained when pushing the head part only against the soft objects. Fig. 10 and Fig. 11 shows the properties. The procedure was the same as the previous experiment where increasing pushing force by 0.25 [N] until the pushing force reached 5 [N]. At every step, pushing distance and force value were recorded and photo (pin image) was taken by camera. The overall procedure was repeated 5 times for every object.

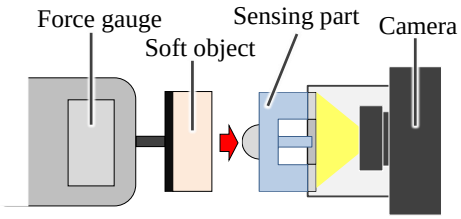

Figure 9. Schematic view of experimental setup for validating the developed stiffness sensing sytem

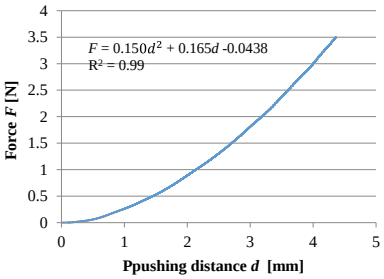

Figure 10. Load versus pushing distance when pushing the head part only against the object made of slicone

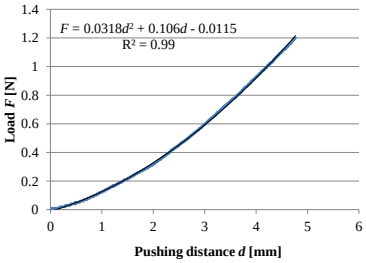

Figure 11. Load versus pushing distance when pushing the head part only against the object made of melamine foam

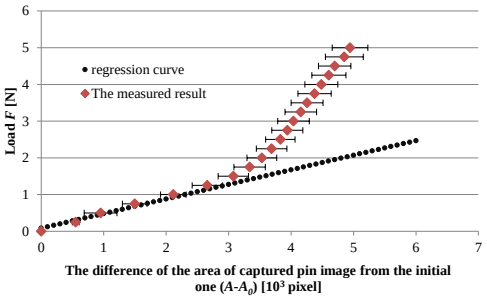

Figure 12. Load versus the difference of the area of captured pin image from the initial one ($A - A_0$) with regression curve when pushing silicone

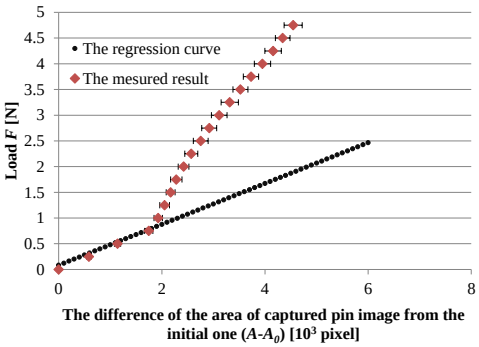

Figure 13. Load versus the difference of the area of captured pin image from the initial one ($A - A_0$) with regression curve when pushing melamine foam

Fig. 12 and Fig.13 shows the relationship between applied load and mean $A - A_0$ with standard deviation. P_c is the point where changes happened, and can be easily detected in Fig. 12 and Fig.13. But we have to know P_c only from $A - A_0$. It is seen that initial several points are on the regression curve, and the force value can be derived from $A - A_0$ before reaching the point P_c. Namely the investigation of increasing pushing force with a step of a certain value without the force gauge (another force sensors) is available. But after reached the point P_c the data points dropped off the regression curve. It is also seen that after reached P_c, the increasing rate of $A - A_0$ decreased; each interval between data points became small. Then, P_c can be detected by letting P_c be the point where the increasing rate of $A - A_0$ changes (when increasing pushing force with a step of a certain value).

According to the procedure for sensing stiffness, the stiffness was calculated. Fig. 14 and Fig. 15 shows the mean derived and actual stiffness with standard deviation. Note that actual stiffness also can deviate due to the change of pushing distance (see Fig.10 and Fig.11), although it is very small. It is seen that in both cases, the stiffness was estimated with small error. But, in case of melamine-foam object, the error was relatively larger. Because the melamine-foam object has small stiffness, the investigation with the step of small force value might be required for getting more accurate stiffness.

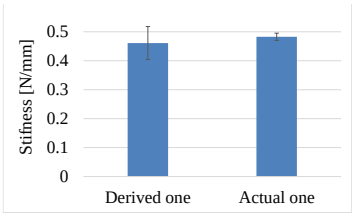

Figure 14. Derived stiffness and actual stifness of silicone object

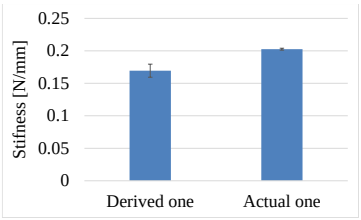

Figure 15. Derived stiffness and actual stifness of melamine-foam object

IV. Conclusion

This research presented novel stiffness sensing system that works by attaching the developed sensing part to the endoscope or camera. If an object or organ touches the sensing part, the pin of the sensing part displaces according to the magnitude of force. By detecting the displacement as visual information, force value can be derived. Additionally the displacement of pin is limited by the structure of spring part. The limitation of the pushing distance can be detected by monitoring the sudden change of increasing rate of pushing distance when pushing object or organ with a step of a certain value of pushing force. The stiffness of object or organ can be derived by deriving the force at the sudden change corresponding to the known limitation of pushing distance. Experimental evaluation showed the validity of the developed system. Remark that experimental results indicated that if investigating the limitation of the pushing distance roughly, the accuracy of the derived stiffness decreased. How to keep accuracy in any case might be our future work.

References

[1] T. Watanabe, T. Iwai, Y. Fujihira, L. Wakako, H. Kagawa and T. Yoneyama, "Force sensor attachable to thin fiberscopes/endoscopes utilizing high elastic fabric," *Sensors*, vol.14, No.3, pp.5207-5220, 2014.

[2] T. Iwai, Y. Fujihira, L. Wakako, H. Kagawa, T. Yoneyama, and T. Watanabe, "Three-axis force visualizing system for fiberscopes utilizing highly elastic fabric," *Proc. of the IEEE/ASME Int. Conf. on Advanced Intelligent Mechatronics (AIM)*, pp.1110-1115, 2014.

[3] P. Puangmali, K. Althoefer, D. Seneviratne, D. Murphy, and P. Dasgupta, "State-of-the-art in force and tactile sensing for minimally invasive surgery," *Sensors Journal*, Vol. 8, No. 4, pp. 371–381, 2008.

[4] E. W. Van der Putten, R. Goossens, J. Jakimowicz, and J. Dankelman, "Haptics in minimally invasive surgery-a review," *Minimally Invasive Therapy & Allied Technologies*, Vol. 17, No. 1, pp. 3–16, 2008.

[5] A. Okamura, C. Verner, and M. Mahvash, "Haptics for robotassisted minimally invasive surgery," *Robotics Research*, 2011, pp. 361–372.

[6] E. V. Poorten, E. Demeester, and P. Lammertse, "Haptic feedback for medical applications, a survey," *Proceedings Actuator*, 2012, pp.18–20.

[7] M. I. Tiwana, S. J. Redmond, and N. H. Lovell, "A review of tactile sensing technologies with applications in biomedical engineering," *Sensors and Actuators A*, Vol. 179, pp. 17-31, 2012.

[8] T. Takaki, Y. Omasa, I. Ishii, T. Kawahara, and M. Okajima, "Force visualization mechanism using a moire fringe applied to endoscopic surgical instruments," *Proc. of IEEE Int. Conf. on Robotics and Automation*, 2010, pp. 3648–3653.

[9] K. Tadano and K. Kawashima, "Development of 4-dofs forceps with force sensing using pneumatic servo system," *Proc. of IEEE Int. Conf. on Robotics and Automation*, 2006, pp. 2250–2255.

[10] J. Peirs, J. Clijnen, D. Reynaerts, H. V. Brussel, P. Herijgers, B. Corteville, and S. Boone, "A micro optical force sensor for force feedback during minimally invasive robotic surgery," *Sensors and Actuators A*, Vol. 115, pp. 447-455, 2004.

[11] T. Kawahara, S. Tanaka, and M. Kaneko, "Non-contact stiffness imager," *Int. J. of Robotics Research*, Vol. 25, No. 5-6, pp.537–549, 2006.

[12] T. Watanabe and Y. Fujihira, "Experimental investigation of effect of fingertip stiffness on friction while grasping an object," *Proc. of IEEE Int. Conf. on Robotics and Automation*, 2014, pp. 889-8943.

[13] Y. Fujihira, K. Harada, T. Tsuji, and T. Watanabe, "Experimental Investigation of Effect of Fingertip Stiffness on Resistible Force in Grasping," *Proc. of IEEE Int. Conf. on Robotics and Automation*, 2014, pp. 4334-4340.